An Analysis of Transient Stresses Produced around Cavities of Arbitrary Shape during the Passage of Traveling Waves

By

Yoshiji NIWA*, Shoichi KOBAYASHI* and Noriaki AZUMA*

(Received September 30, 1974)

(Summary)

The present paper is concerned with an application of the integral equation method to the analysis of the transient stresses produced around cavities of arbitrary shape, which are excavated in an infinite elastic medium and subject to longitudinal and transverse waves of arbitrary pressure-time history. The method used in the present paper consists of such a technique as devising a solution for the transient problem from the superposition of appropriate steady-state solutions, which are obtained by use of the integral equation.

The validity of the present method is demonstrated by several examples such as : (1) steady-state stresses around a circular cavity due to longitudinal and transverse waves, (2) transient stresses around a circular cavity due to step-form longitudinal and transverse waves, and a triangular-form longitudinal wave, (3) transient stresses around a horseshoe-shaped cavity due to a step-formed longitudinal wave.

It may be concluded that the present method is advantageously applied to transient problems, specifically with boundaries of arbitrary shape and accompanied also with traveling waves of arbitrary pressue-time history.

1. Introduction

From the anti-seismic and anti-blasting desingn point of view, it is of basic importance to accumulate knowledge about transient behaviors of a structure-surrounding-medium system impinged upon by traveling waves. Although an exact analysis of such behaviors of the system is rather difficult, approximate numerical analyses may be quite satisfactorily applied with appropriate idealizations of the concerned system[1]. In most cases, an underground structure-surrounding-medium system may well be idealized as a cavity excavated in the elastic medium, which is also an extreme case of the real structure-medium system.

The present paper is concerned with an application of the integral equation

* Department of Civil Engineering.

method to the analysis of the transient stresses produced around cavities of an arbitrary shape during the passage of traveling waves of an arbitrary pressure-time history. The subject matter of the present paper was partially studied by a number of investigators[1)~5)]. The difraction of a transient pressure pulse by a cylindrical cavity in an infinite elastic medium was analysed by the use of integral transform or related techniques[2)~4)], or the superposition of appropriate steady-state solutions[5)]. The former techniques usually lead to formidable difficulties in the inversion process, whereas the latter is far simpler when the construction of a train of pulse of traveling waves is possible from the steady-state sinusoidal components. Each pulse represents, with sufficient accuracy, the time history of the transient stresses in the incident wave.

The use of a steaby-state solution to obtain a transient response has been suggested by Bisplinghoff, Isakson and Pian[6)]. The validity of the method was demonstrated slso in the reference[5)].

The method used in the present paper consists of such a technique as devising a solution for the transient problem from the superposition of appropriate steady-state harmonic solutions to the Helmholtz equations. These are obtained by the integral equation method, which can be applied to any problems of an arbitrary shape of boundary. The accuracy of the solution obtained by the present method may be improved as much as is desired by choosing correspondingly many steady-state solutions and boundary points used in the numerical procedures of the integral equation. Since all the operations in the present method are performed in the physical plane, the direct physical insight into the problem may be easily obtained.

2. Integral equation method

Fundamental equations, i. e., equations of motion, constitutive equations, and strain-displacement relations, of homogenous and isotropic linear elastic solid are expressed in a rectangular cartesian coordinate system (x_1, x_2, x_3) as follows:

$$\tau_{ji,j}+f_i=\rho\ddot{u}_i \quad \cdots\cdots(1)$$

$$\tau_{ij}=\lambda\varepsilon_{kk}\delta_{ij}+2\mu\varepsilon_{ij} \quad \cdots\cdots(2)$$

$$\varepsilon_{ij}=\frac{1}{2}(u_{i,j}+u_{j,i}) \quad \cdots\cdots(3)$$

where τ_{ij}, ε_{ij}, u_i, f_i and δ_{ij} imply the stress tensors, strain tensors, displacement vectors, body force vectors and Kronecker's delta, respectively, λ and μ represent Lamé constants and ρ the density of the solid. The comma and dot notations imply the partial differentiation with respect to the following index and time, respectively, i. e., $\tau_{ji,j}\equiv\partial\tau_{ji}/\partial x_j$ and $\ddot{u}_i\equiv\partial^2u_i/\partial t^2$. Further, the indices cover range 1, 2, 3; and the summation convention rule is also applied.

Equations of motion are also expressed in terms of displacements by substituting from Eqs. (2) and (3) into Eq. (1)

$$(\lambda+\mu)u_{j,ji}+\mu u_{i,jj}+f_i=\rho\ddot{u}_i \quad \cdots\cdots(4)$$

These are the fundamental equations called Navier-Cauchy equations.

Now we assume that the whole system or the elastic solid is the state of steady harmonic motion and the body forces may be neglected. The space and time variables, thus, may be separated

$$u_j(x_i,\ t)=Re\{\bar{u}_j(x_i)e^{-i\omega t}\} \quad \cdots\cdots(5)$$

where $\bar{u}_j\ (x_i)$ are functions of space variables only, and Re means to take the real part of the quantities, and ω is the circular frequency different from eigenfrequencies.

The Navier-Cauchy equations (4) are thus transformed by substituting from Eq. (5) to

$$(c_1^2-c_2^2)\bar{u}_{j,ij}+c_2^2\bar{u}_{i,jj}+\omega^2\bar{u}_i=0 \quad \cdots\cdots(6)$$

where

$$c_1^2=\frac{\lambda+2\mu}{\rho} \quad \text{and} \quad c_2^2=\frac{\mu}{\rho} \quad \cdots\cdots(7)$$

imply the squared velocities of the longitudinal and transverse waves, respectively.

We now introduce a new operator Δ^* defined as

$$\Delta^*\equiv(c_1^2-c_2^2)\text{grad}\,\nabla\cdot+c_2^2\nabla^2=(c_1^2-c_2^2)\partial_j e_j\partial_i e_i\cdot+c_2^2\partial_j\partial_j \quad \cdots\cdots(8)$$

where $\nabla=\partial_i e_i$ and e_i are unit vectors in the coordinate directions, ∂_i mean partial differentiation with respect to the index. Eq. (6) is thus expressed in a vector form as (bars are ommitted hereafter for the sake of simplicity)

$$(\Delta^*+\omega^2)\boldsymbol{u}=\boldsymbol{L}\boldsymbol{u}=0 \quad \cdots\cdots(9)$$

$$\text{with} \quad \boldsymbol{L}=\Delta^*+\omega^2 \quad \cdots\cdots(10)$$

This is the fundamental equation to be solved with appropriate boundary conditions, and is called Helmholtz equation.

We shall next transform the fundamental differential equations into a system of integral equations.

Suppose now two displacement vectors $\boldsymbol{u}$ and $\boldsymbol{v}$, which satisfy Eq. (9) in the domain D and its boundary S as shown in Fig. 1. Then assume that their partial derivatives up to the second order are continuous in $D+S$. Utilizing the Green's identity, the following relation can be obtained after some manipulation

$$\int_V(\boldsymbol{v}\cdot\boldsymbol{L}\boldsymbol{u}-\boldsymbol{L}\boldsymbol{v}\cdot\boldsymbol{u})dv=\int_S\{\boldsymbol{v}\cdot\boldsymbol{T}^n\boldsymbol{u}-(\boldsymbol{T}^n\boldsymbol{v})^T\cdot\boldsymbol{u}\}ds \quad \cdots\cdots(11)$$

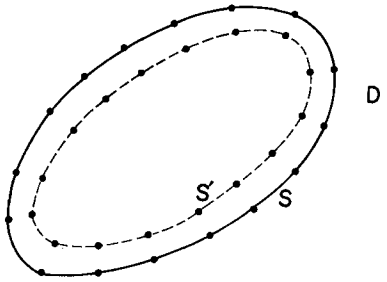

Fig. 1 Exterior domain D and its boundary S, and auxiliary boundary S'.

where

$$\boldsymbol{T}^n\boldsymbol{u}=(c_1^2-2c_2^2)\boldsymbol{n}\mathrm{div}\boldsymbol{u}+2c_2^2\boldsymbol{n}\cdot\mathrm{grad}\boldsymbol{u}+c_2^2(\boldsymbol{n}\times\mathrm{rot}\boldsymbol{u}) \quad \cdots\cdots(12)$$

and $\boldsymbol{n}$ is a unit outward normal vector on S.

We here consider the following differential equation corresponding to Eq. (9)

$$\boldsymbol{L}\boldsymbol{\Gamma}(P;Q)=-\delta(P;Q) \quad \cdots\cdots(13)$$

where P (x_1, x_2, x_3) and Q (y_1, y_2, y_3) are called observation point and source point, respectively, and $\delta(P;Q)$ means a delta function defined as $\delta(P;Q)=\delta(x_1-y_1)\ \delta(x_2-y_2)\ \delta(x_3-y_3)$. The solution which satisfies Eq. (13) is called a fundamental solution or elementary solution, which is equivalent to Green's function in an infinite domain.

The substitution of $\boldsymbol{u}$ and $\boldsymbol{\Gamma}$ for $\boldsymbol{u}$ and $\boldsymbol{v}$, respectively, in Eq. (11) leads to the following integral equation

$$\boldsymbol{u}(P)F(P)=\int_S\{\boldsymbol{\Gamma}(P;R)\cdot\boldsymbol{T}^n\boldsymbol{u}(R)-[\boldsymbol{T}^n\boldsymbol{\Gamma}(R;P)]^T\cdot\boldsymbol{u}(R)\}ds \quad \cdots\cdots(14)$$

where

$$F(P)=\begin{cases}1 & \text{for } P\in D\\ \dfrac{1}{2} & P\in S\\ 0 & P\notin D,\ P\notin S\end{cases} \quad \cdots\cdots(15)$$

and $R\in S$, that is, P is a point either in the domain, on the boundary, or not, whereas R is a point always on the boundary. Eq. (14) is a basic integral equation corresponding to the differential equation (9). Since the fundamental solution $\boldsymbol{\Gamma}$ may be easily obtained, Eq. (14) is reduced to a system of integral equations with a singular kernel with respect to the unknown function $\boldsymbol{u}$. The system of integral equations may somehow be solved, then displacements and thus stresses at any points shall be easily determined.

Hereafter, we restrict ourselves to problems in the state of plane strain unless otherwise mentioned. In the state of plane strain, the fundamental solution can

be easily obtained by taking account of the Sommerfeld radiation condition. The solution, i. e., the Green tensor, can be expressed by a matrix of two by two. The elements of the matrix Γ_{ik} are obtained as follows:

$$\Gamma_{jk}=\frac{i}{4\mu}\left[H_0^{(1)}(\xi_2 r)\delta_{jk}-\frac{1}{\xi_2^2}\frac{\partial^2}{\partial x_j \partial x_k}\left\{H_0^{(1)}(\xi_1 r)-H_0^{(1)}(\xi_2 r)\right\}\right] \cdots\cdots (16)$$

where $\xi_1=\omega/c_1$, $\xi_2=\omega/c_2$, $r=\overline{PQ}=\sqrt{(x_i-y_i)(x_i-y_i)}$,

and $H_0^{(1)}(\xi_n r)$ implies the zero order Hankel function of the first kind with an argument $\xi_n r$.

3. Statement of problems and applied technique

Although the integral equation method mentioned above may be applied to any kind of bounbry value problems, we shall deal with stress boundary problems in the state of plane strain. These would include long cavities excavated in an infinite elastic solid impinged upon by plane longitudinal and transverse waves of arbitrary pressure-time history, traveling in the direction perpendiculart to the axis of the cavities.

The method of solution of the problems presented in this paper consists of three steps. The first is to approximate the transient longitudinal and transverse waves of arbitrary pressure-time history by the Fourier series. The second is to obtain the steady-state solutions of the respective sinusoidal waves by use of the integral equation method. The third is to superpose the solutions in such a way as the original traveling waves are constructed.

In the first step, in order to meet the initial traction free condition at the boundary of cavities, care must be taken to choose enough time between pulses to allow the surface energy to be dispersed into the surrounding medium. The accuracy of the Fourier series must be also checked in comparison with the incident waves. The most stringent example is a step-form wave, which is illustrated in Fig. 2, i. e., the Fourier series expansion with ten terms superposed.

In the second step, it is rather difficult to solve the system of integral equations analytically even in a simple case. Thus, we are forced to treat the system by numerical procedures.

Let the boundary S be divided into N subdivisions and the values $\boldsymbol{u}(R)$, $\boldsymbol{\Gamma}(P;R)$ be assumed constant throughout the subdivision. Eq. (14) can be approximated by the following algebraic equations

$$\frac{1}{2}\boldsymbol{u}(R_m)=\sum_{n=1}^{N}\boldsymbol{T}^n\boldsymbol{u}(R_n)\int_S \boldsymbol{\Gamma}(R_n, R_m)ds-\sum_{n=1}^{N}\boldsymbol{u}(R_n)\int_S[\boldsymbol{T}^n\boldsymbol{\Gamma}(R_n, R_m)]^T ds \cdots (17)$$

where R_m and R_n imply the midpoints of the subdivision. In the types of

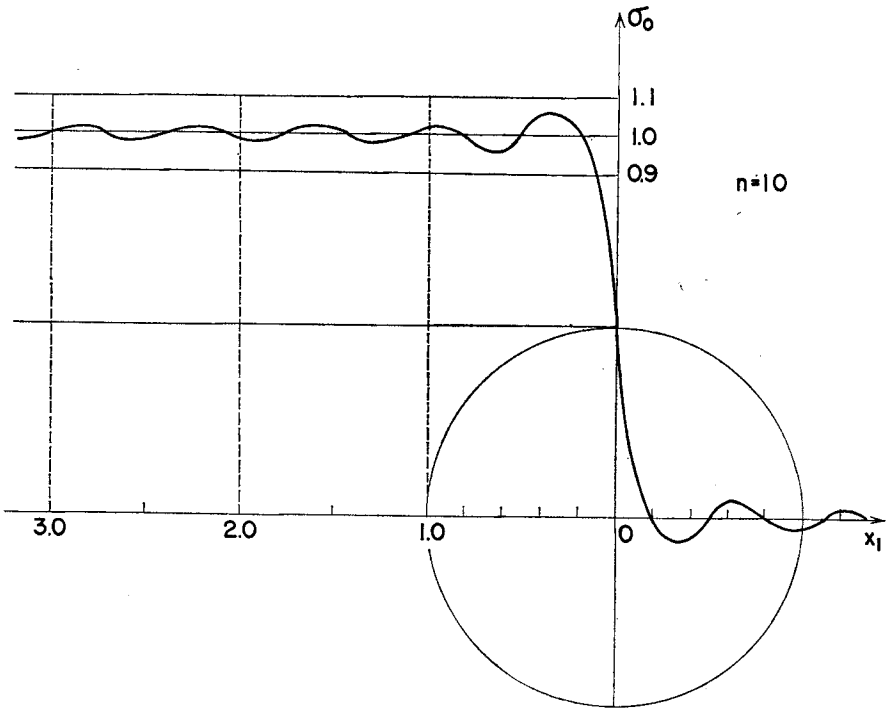

Fig. 2 Fourier expansion of step-form pulse with ten terms.

problems considered in the present paper, the solution shall be conveniently expressed by using a type of single-layer potential[7] with a density $\varphi(Q)$ such as

$$\boldsymbol{u}(P)=\int_S \boldsymbol{\Gamma}(P;\,Q)\varphi(Q)ds \quad \cdots\cdots(18)$$

with the boundary condition

$$\boldsymbol{T}^n\boldsymbol{u}(R)=\boldsymbol{g}(R),\ R\in S \quad \cdots\cdots(19)$$

Eq. (14), therefore, is reduced to

$$\boldsymbol{g}(R)=\frac{1}{2}\varphi(R)+\int_S \boldsymbol{T}^n\boldsymbol{\Gamma}(Q;\,R)\varphi(Q)dS \quad \cdots\cdots(20)$$

or is approximated by the expression, noting $\boldsymbol{\Gamma}(R;\,Q)=\boldsymbol{\Gamma}(Q;\,R)$,

$$\boldsymbol{g}(R_n)=\frac{1}{2}\varphi(R_n)+\sum_{n=1}^{N}\varphi(Q)\int_S \boldsymbol{T}^n\boldsymbol{\Gamma}(Q;\,R_n)dS \quad \cdots\cdots(21)$$

where R_n implies the midpoint of the subdivision.

In the numerical procedures, it is more desirable to introduce an approximate auxiliary boundary, and transform the system of singular integral equations into an equivalent system of regular integral equations.

Let us now introduce an appropriate auxiliary boundary and approximate it

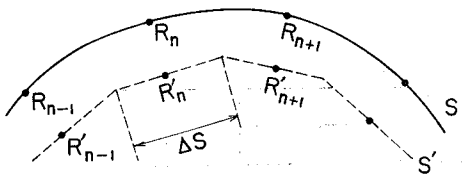

Fig. 3 Boundary S and corresponding auxiliary polygonal boundary S'. Part of them are shown.

by an appropriate polygon, as partly shown in Fig. 3, and then assume that the density $\varphi(R')$ is constant throughout the subdivision. Eq. (21) may be transformed to

$$\boldsymbol{g}(R_m)=\sum_{n=1}^{N}\varphi(R_n')\int_S \boldsymbol{T}^n\boldsymbol{\Gamma}(R_n';R_m)\,dS \quad \cdots\cdots(22)$$

where R_m and R_n' imply midpoints of the subdivision of the real boundary and the auxiliary boundary, respectively.

Eq. (22) can be easily solved for the density $\varphi(R_n')$. Then, displacements and also stresses at an arbitrary point may be obtained, respectively, by the use of Eq. (18) and Eqs. (2) and (3). The procedure of superposition of steady-state solutions thus obtained is straightforward. The Duhamel integral procedure, i. e., numerical integration in the present case, is also applicable, if transient solutions due to traveling unit step-form waves are available at an appropriate series of time.

4. Numerical examples

4.1 Steady-state stresses around a circular cavity

(A) Stresses due to longitudinal wave

In order to test the accuracy of the numerical procedures of the integral equation method, steady-state stresses around a circular cavity due to longitudinal plane displacement waves were calculated and compared with the solutions obtained by Pao[8] by use of the eigen-expansion method.

The incident plane displacement wave considered is expressed by

$$u_1^{(k)}=Ae^{i(\alpha x_1-\omega_1 t)},\qquad \alpha=\frac{\omega_1}{c_1}=\frac{2\pi}{l_1} \quad \cdots\cdots(23)$$

where A, α, ω_1, and l_1 represent the amplitude, wave number, circular frequency of the wave and wave length, respectively.

The problem analysed is a circular cavity in an infinite elastic plate of plane-stress state, as shown in Fig. 4, with its auxiliary boundary and corresponding

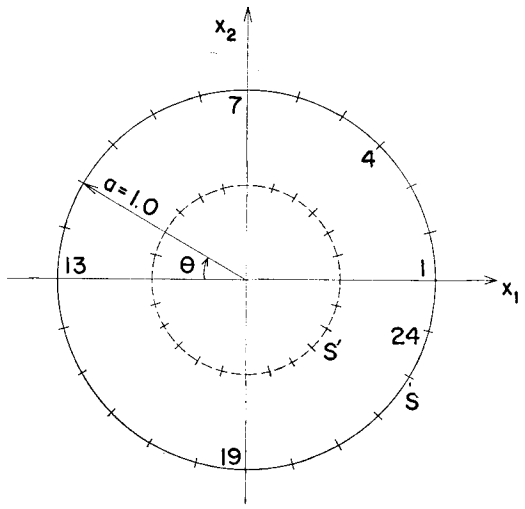

Fig. 4 A circular cavity in an infinite elastic medium and its auxiliary boundary and boundary points, used in the numerical procedures.

boundary points. The accuracy of the numerical results, which is influenced by the selection of the auxiliary boundary and its boundary points, was discussed elsewhere[9], and found to be appropriate in the present case to choose the points in such a way as shown in the figure.

The numerical results of circumferential stresses on the boundary of the cavity are shown in Fig. 5, in comparison with Pao's results[8], where a, σ_0 and T mean the radius of the cavity with $a=1.0$, the maximum value of stress due to the plane displacement wave and the period of the wave, respectively. Pisson's ratio was assumed $\nu=0.35$. Both results show an excellent agreement.

As the wave length increases, the stress distribution approaches that of the static case. When the wave length decreases, a scattering of waves reduces overall stress concentration.

Similar results obtained in the state of plane strain with Poisson's ratio $\nu=0.25$ are again shown in Fig. 6. The accuracy of the numerical results may progressively decrease for waves with a short wave length, because the limited number of boundary points selected may not be enough to fully reproduce the wave form.

(B) Steady-state stresses due to transverse wave

Steady-state stresses on the boundary of a circular cavity in the state of plane strain due to transverse displacement waves are shown in Fig. 7, where τ_0 and T are the maximum shear stress due to the transverse displacement wave and the period of the wave, respectively. The incident transverse wave is expressed in the same way as the longitudinal wave

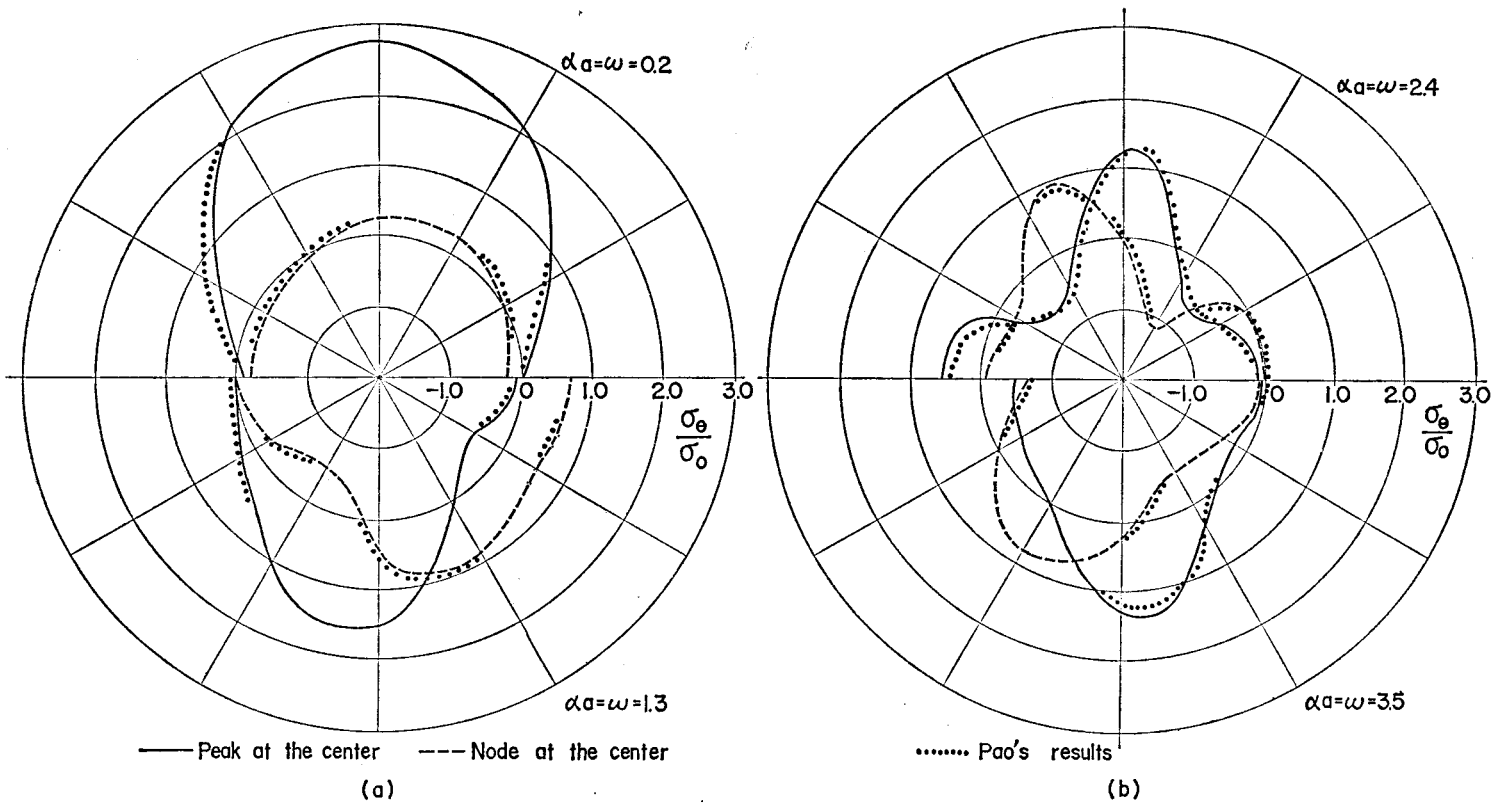

Fig. 5 Circumferential stresses on the boundary of the cavity due to longitudinal sinusoidal wave compared with Pao's results (in the state of plane stress).

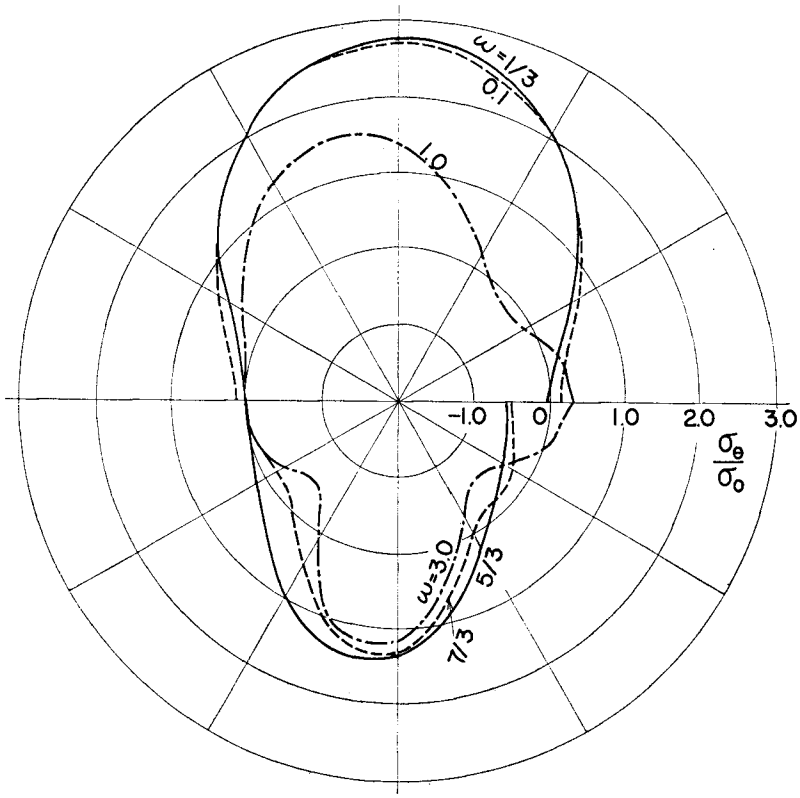

Fig. 6 Circumferential stresses on the boundary of the cavity due to longitudinal sinusoidal wave (in the state of plane strain).

$$u_2^{(k)} = Be^{i(\beta x_1 - \omega_2 t)}, \quad \beta = \frac{\omega_2}{c_2} = \frac{2\pi}{l_2} \qquad \cdots\cdots(24)$$

where B, β, ω_2 and l_2 represent the amplitude, wave number, circular frequency of the wave and wave length, respectively. In the numerical procedures, the similar auxiliary boundary as shown in Fig. 4 but 48 boundary points were chosen and the Poisson's ratio is $\nu=0.25$.

As the wave length increases, the shape of stress distribution becomes similar to that in the static case, but slightly larger, as might be expected. The scattering effect becomes increasingly predominant as the wave length decreases. When the wave length becomes so short as to be comparable to the distance between the adjacent points on the boundaty, the accuracy of the results may be questionable. It is a quite difficult problem to select boundary points in order to guarantee a certain accuracy of the results. As a whole, it may safely be said the more points are selected on the boundary and the more apart auxiliary boundary from the real boundary is chosen as far as solvable of the problem, the more accuracy can be expected.

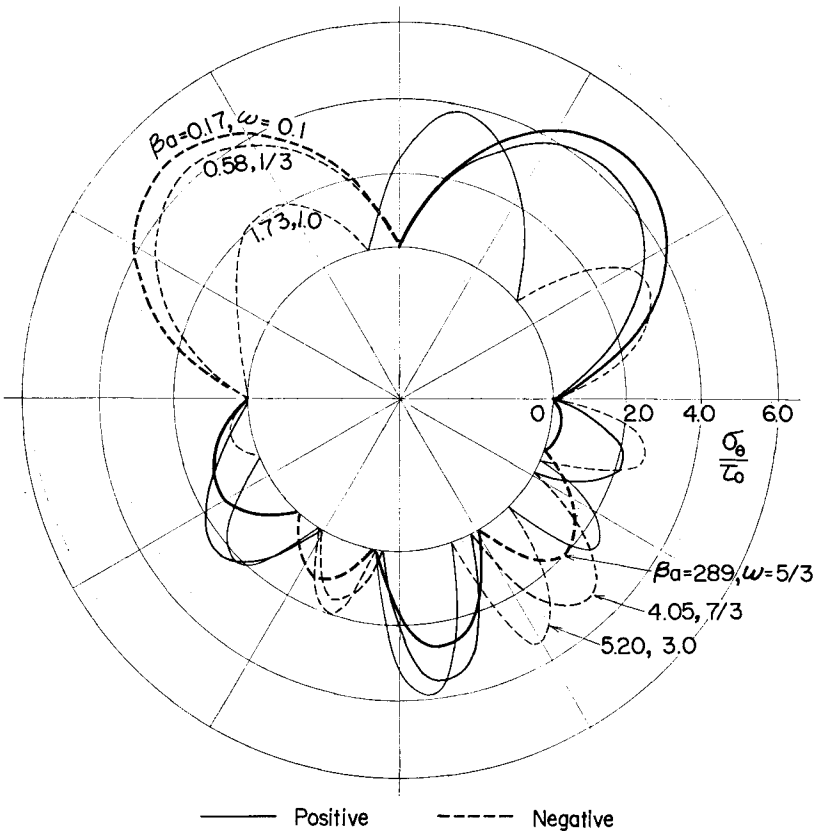

Fig. 7 Circumferential stresses on the boundary of the cavity due to transverse sinusoidal wave.

4.2 Transient Stresses around a circular cavity

(A) Stresses due to longitudinal waves

Transient stresses due to a traveling wave are easily constructed from the stresses of steady-state, such as those obtained a bove by the use of the principle of superposition as mentioned in section **3**.

The most fundamental and valuable state of stresses is that which is due to a step-form traveling wave. Thus, transient stresses due to such a longitudinal traveling wave are obtained as a first example. In advance, to show the results, it should be noticed that the tremors remain unswept in the traction free period following each pulse, which are influenced, of course, by the approximation of the wave by Fourier expasnion as shown in Fig. 2. The tremors shown in Fig. 8 correspond to just the instant at which the incident pulse arrives at the left boundary of the cavity. As the traction free interval becomes large enough, the

magnitude of the tremors naturally decreases.

In the following examples, the Fourier expansion with period 6π and terms up to the tenth are used.

Fig. 9 shows the transient circumferential stresses on the boundary of the circular cavity, where different types of curves correspond to the respective positions of the wave front relative to the cavity as shown in the small figure.

The circumferential stress at point $\theta=90°$, due to the incident step-form longitudinal wave, is shown in Fig. 10 with the results by Garnet and Pascal[5], where time t is taken to be zero at the moment at which the wave front arrives at the

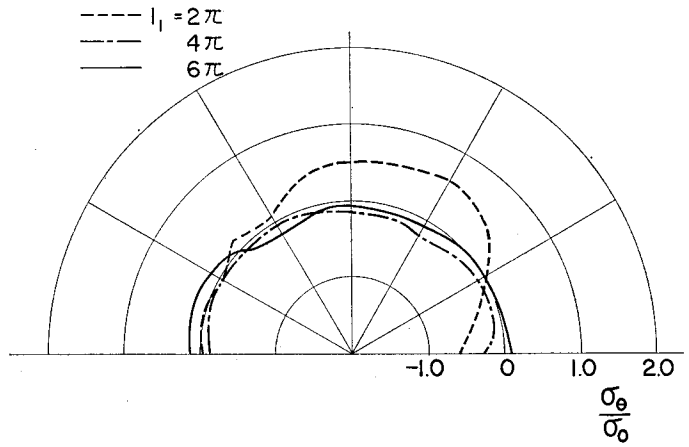

Fig. 8 Tremors due to fluctuations of approximated longitudinal wave by Fourier expansion and precurssion wave, at the instant at which the wave front arrives at the left boundary of the cavity.

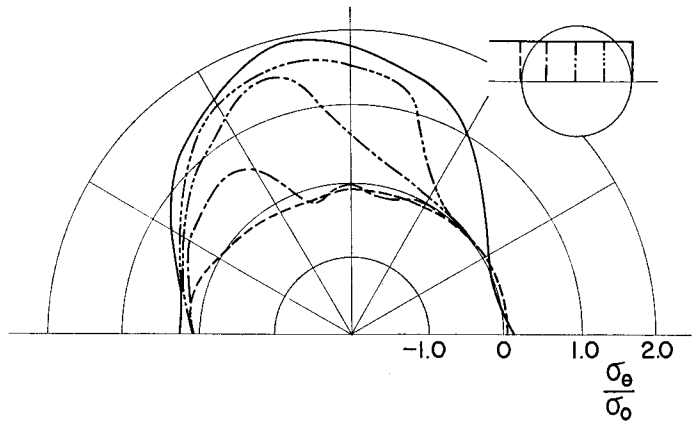

Fig. 9 Transient circumferential stresses on the boundary of the cavity due to a longitudinal step-form wave corresponding to the indicated positions of wave front.

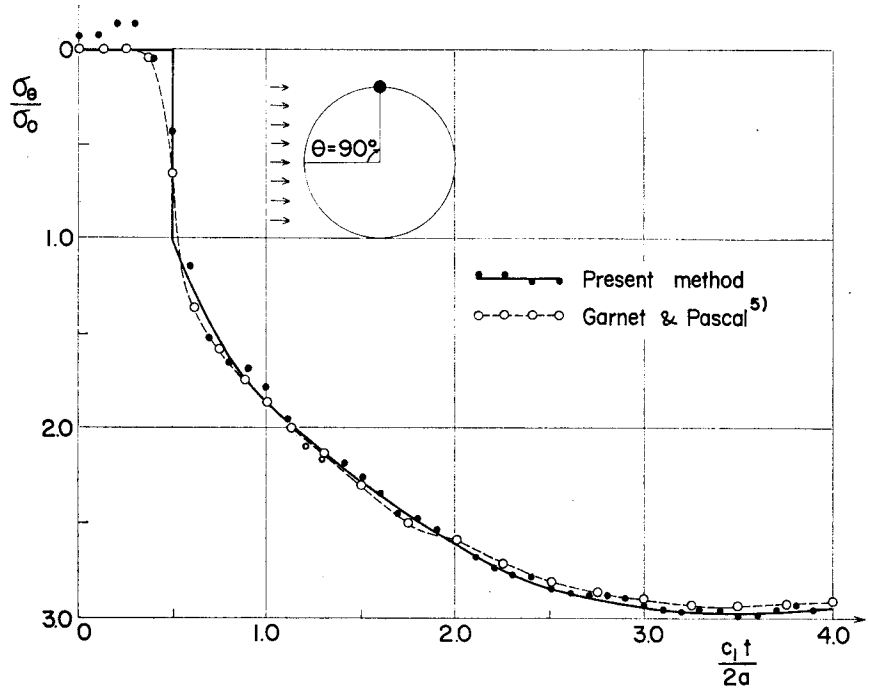

Fig. 10 Circumferential stress-time history at a point $\theta=90°$ on the boundary of the cavity due to longitudinal step-form wave. Time t is taken zero at the instant at which the wave front arrives at the left boundary.

left boundary of the cavity. In the curve of the present method, the small fluctuations caused by the approximation of the wave by the Fourier expansion (see Fig. 2) are reasonably eliminated. The maximum circumferential stress appears at the nondimensional time 3.5 and its value is about -2.98, whereas it is -2.67 in the static case.

The circumferential stress at point $\theta=0°$, due to the incident longitudinal step-form pulse, is also shown in Fig. 11. The results obtained by the present method show some disagreement with the results by Garnet and Pascal[5], especially in the range of small values of the non-dimensional time. The reason is not clear, but may be found in the difference of the Poisson's ratios in the both cases. The transient maximum stress concentration is about 0.22 at 1.5 of the nondimensional time, whereas it is zero in the static case.

The second example is of circumferential stresses produced on the boundary of the cavity during the passage of a triangular longitudinal traveling wave. The results are shown Fig. 12, where each type of line corresponds respectively to the instantaneous positions of the wave as shown in the small figure. The maximum stress is observed to follow just after the peak of the traveling wave.

The stress-time history of a fixed point at the boundary of the cavity may easily be constructed by the Duhamel integral procedure, using the results due to the step-form traveling wave, such as shown in Fig. 10, for example. The prelim-

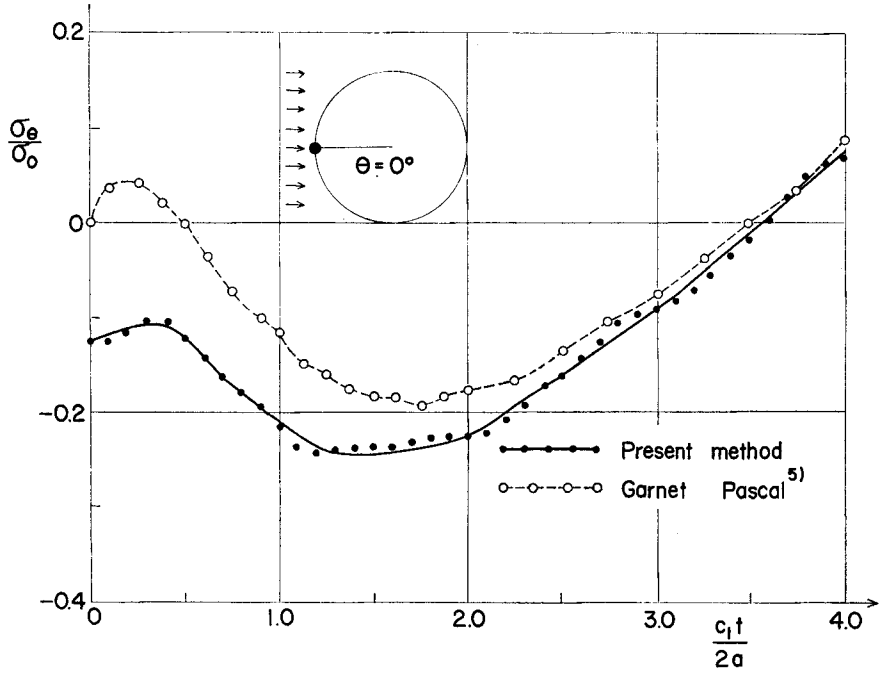

Fig. 11 Circumferential stress–time history at a point $\theta=0°$ on the boundary of the cavity due to a longitudinal step–form wave. Time t is taken zero at the instant at which the wave front arrives at the left boundary.

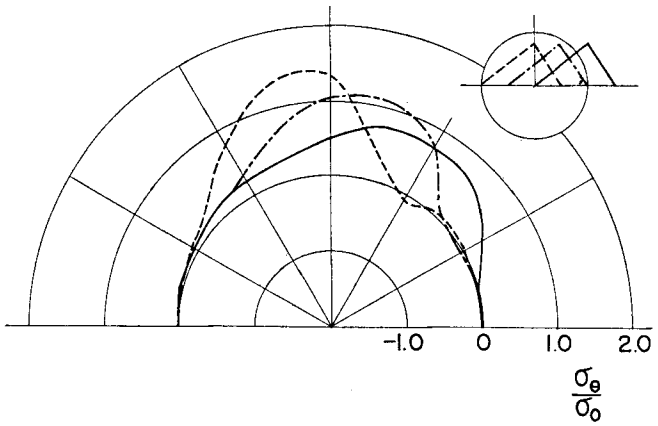

Fig. 12 Transient circumferential stresses on the boundary of the cavity due to a longitudinal triangular wave, corresponding to the indicated positions of the wave.

inary test of the stress at the boundary at point $\theta=90°$ revealed that the stress constructed by the Duhamel integral (summation in this case) with ten steps, agreed with that by the direct Fourier expansion of the wave within 4 percent errors. Thus, it may be concluded that the stress-time history at the boundary point at $\theta=90°$ and 0°, due to any form of traveling waves, is easily constructed with a sufficient accuracy.

The third example is of the circumferential stresses on the boundary of the circular cavity, due to a single traveling pulse of the longitudinal sine wave. The results are shown in Fig. 13, with the respective positions in the small figure. These results are compared with those due to the harmonic trains of the same

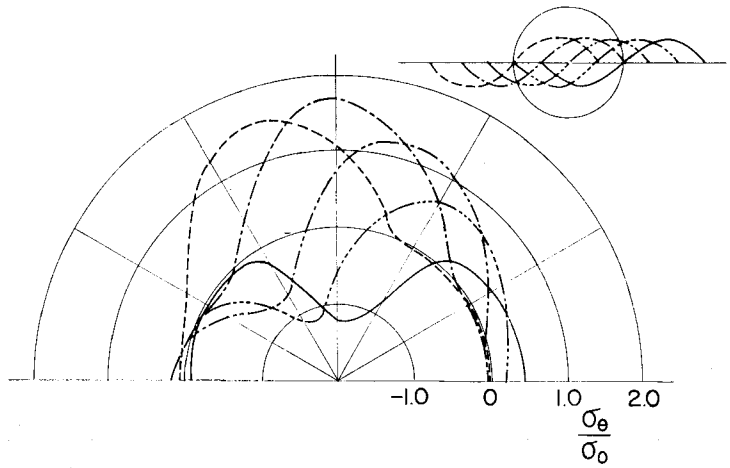

Fig. 13 Transient circumferential stresses on the boundary of the cavity due to a longitudinal single sine pulse corresponding to the indicated positions of the wave.

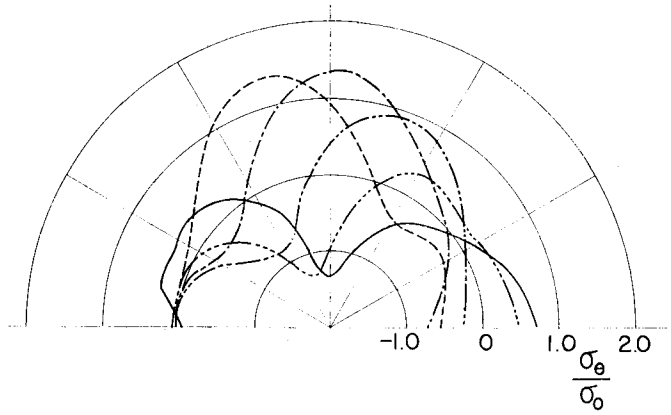

Fig. 14 Circumferential stresses on the boundary of the cavity due to longitudinal sinusoidal wave train, each position of the peak corresponds to a single sine pulse shown in Fig. 13.

wave and at the same positions, as shown in Fig. 14. It may safely be said that the transient stress concentration due to the first half-sine wave is slightly higher than that due to the harmonic wave with the same amplitude. On the other hand, the stress concentration due to the second half-sine wave is slightly lower than that due to the harmonic wave.

(B) Stresses due to transverse wave

Transient stresses due to a traveling transverse wave are analysed in a similar manner as mentioned above in the case of longitudinal waves.

The transient stresses due to a traveling step-form pulse with several relative positions to a circular cavity are shown in Fig. 15. The tremors just in advance of the incident wave may not be very small, which are caused by the selection of

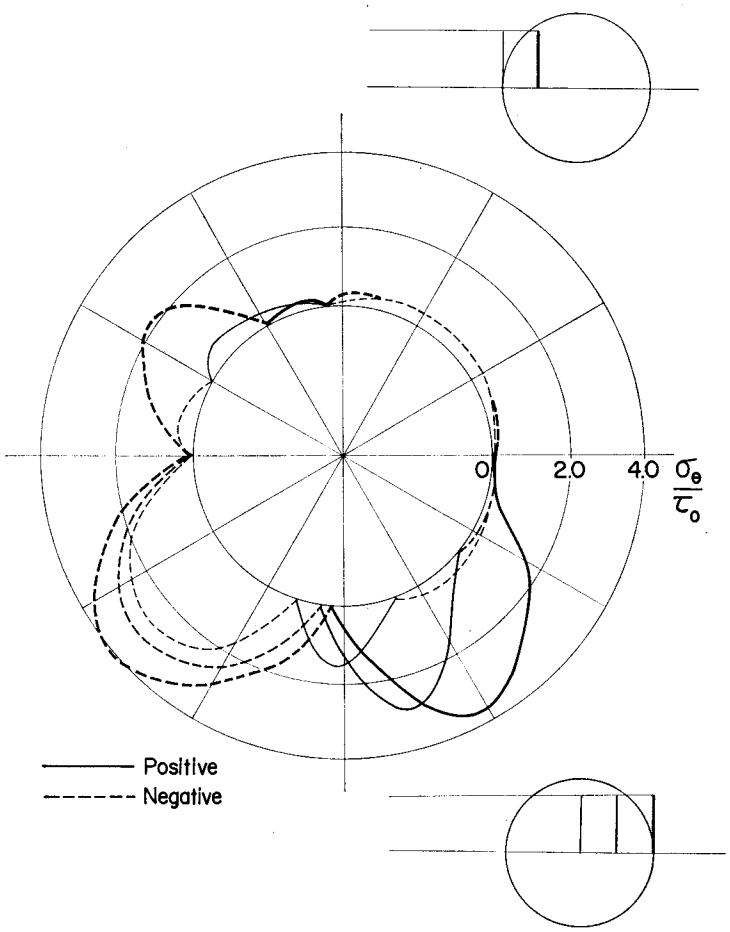

Fig. 15 Transient circumferential stresses on the boundary of the cavity due to a transverse step-form wave corresponding to the indicated positions of the wave.

the Fourier expansion period and precussion wave. In this case, the period was chosen $l_2=6\pi c_2=3.46\pi$, which is about half of that in the longitudinal wave. Because of the fading effect of the precursive wave, the tremors are maximum at the position of the wave shown top in Fig. 15. Thus, the maximum error in the results may be ten percent at most.

The circumferential stress-time history of the boundary at $\theta=45°$ is shown in Fig. 16, where time t is taken to be zero at the moment at which the wave front arrives at the left boundary of the cavity. The small fluctuations due to the approximation of the step-form wave and the precursion wave are eliminated by a simple observation. The transient stress concentration increases with an increase of the nondimensional time passed up to about 5.2 at time t=2.5, whereas it is 4.0 in the static case.

Stress concentration at the point $\theta=45°$, due to any form of traveling transverse waves, may also be obtained by the Duhamel integral procedure as in the case of longitudinal waves mentioned in the previous section.

4.3 Transient stresses around a cavity of arbitrary shape

The most important merit of the present method over other semi-analytical

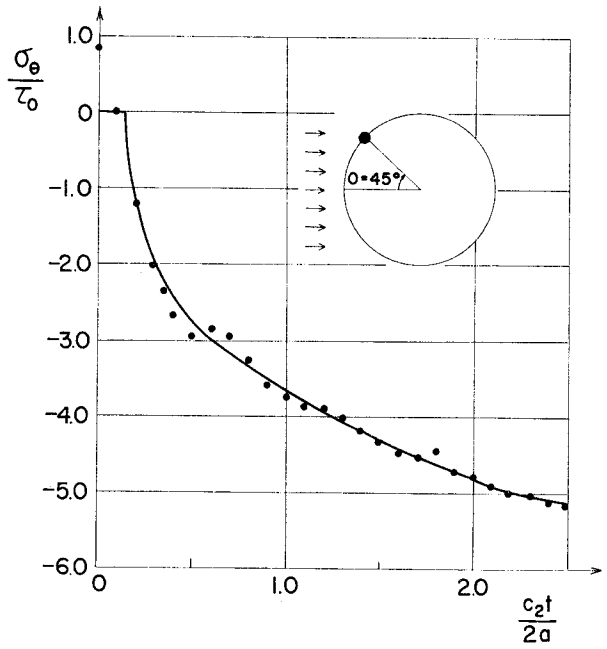

Fig. 16 Circumferential stress-time history at a point $\theta=45°$ on the boundary of the cavity due to transverse step-form wave. Time t is taken zero at the instant at which the wave front arrives at the left boundary.

methods is that it is applicable to any problem with a boundary of arbitrary shape with equal ease. As a typical example, transient stresses on the boundary of a horseshoe-shaped cavity during the passage of a longitudinal step-form pulse traveling in a horizontal direction have been analysed, and are shown in Fig. 17.

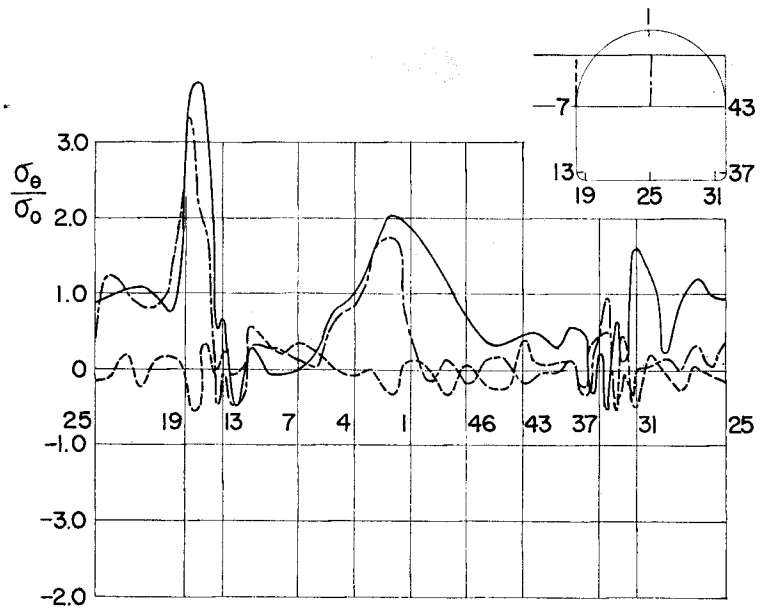

Fig. 17 Transient circumferential stresses on the boundary of the horseshoe-shaped cavity due to a traveling longitudinal step-form wave, corresponding to the indicated positions of wave front.

It is observed that high stress concentration occurs at the rounded toe corners with a small radius, and also at the crown of the arch section. However, the transient stress concsntration is not so high as compared with that of the static case obtained elsewhere[9].

The more complicated problems may be similarly treated with ease, although it is recommended to check the accuracy by comparing the results obtained by selecting several different auxiliary boundaries and boundary points as well.

5. Concluding remarks

The validity and the availability of the present integral equation method for a transient analysis of stresses during the passage of traveling waves may be confirmed by several examples.

Although there remain some ambiguities about the estimation of errors in the numerical procedures, the present method may be advantageously applied to tran-

sient problems, specifically with a boundary of arbitrary shape and accompanied with arbitrary-formed traveling waves.

Acknowledgement

The numerical computations were performed on FACOM 230-75, at the Data processing Center of Kyoto Univeristy.

References

1) Niwa, Y., S. Kobayashi and T. Mastumoto ; J. Soc. Material Sci., vol. 23, pp. 361-367, 1974 (in Japanese)
2) Baron, M. L. and A. T. Matthews ; J. Appl. Mech., vol. 28, pp. 347-354, 1961
3) Baron, M. L. and R. Parnes ; J. Appl. Mech., vol. 29, pp. 385-395, 1962
4) Peralta, L. A., G. F. Carrier and C. C. Mow ; J. Appl. Mech., vol. 33, pp. 168-172, 1966
5) Garnet, H. and J. C-Pascal ; J. Appl. Mech., vol. 33, pp. 521-531, 1966
6) Bisplinghoff, R. L., G. Isakson and T. H. Pian ; J. Aeronaut. Sci., vol. 17, 1950
7) Kupradze, V. D. ; Potential Methods in the Theory of Elasticity, transl. by Gutfreund, Israel Program for Scientific Translations, Jerusalem, 1965
8) Pao, Y.-H. ; J. Appl. Mech., vol. 29, pp. 299-305, 1962
9) Niwa, Y., S. Kobayashi and K. Yokota ; Trans. Japan Soci. Civil Eng., no. 195, pp. 27-35, 1971 (in Japanese)